JOURNAL OF BACTERIOLOGY, Aug. 1997, p. 4963–4969 Vol. 179, No. 16
0021-9193/97/$04.00+0

Cell Cycle Characteristics of Thermophilic Archaea

ROLF BERNANDER* AND ANDRZEJ POPLAWSKI

Department of Microbiology, Biomedical Center, Uppsala University, S-751 23 Uppsala, Sweden

Received 26 March 1997/Accepted 5 June 1997

We have performed a cell cycle analysis of organisms from the *Archaea* domain. Exponentially growing cells of the thermophilic archaea *Sulfolobus solfataricus* and *Sulfolobus acidocaldarius* were analyzed by flow cytometry, and several unusual cell cycle characteristics were found. The cells initiated chromosome replication shortly after cell division such that the proportion of cells with a single chromosome equivalent was low in the population. The postreplication period was found to be long; i.e., there was a considerable time interval from termination of chromosome replication until cell division. A further unusual feature was that cells in stationary phase contained two genome equivalents, showing that they entered the resting stage during the postreplication period. Also, a reduction in cellular light scatter was observed during entry into stationary phase, which appeared to reflect changes not only in cell size but also in morphology and/or composition. Finally, the in vivo organization of the chromosome DNA appeared to be different from that of eubacteria, as revealed by variation in the relative binding efficiency of different DNA stains.

The *Archaea* domain was recognized as a separate evolutionary lineage around 1977 (20), and the archaea may even be more closely related to eukaryotes than to other prokaryotes. With the complete genome sequencing of the archaeon *Methanococcus jannaschii* (4), a fascinating combination of features from the *Bacteria* and *Eucarya* domains was revealed, and the evolutionary uniqueness of the *Archaea* domain was confirmed.

The metabolic and biochemical properties of different archaeal species have been extensively studied, but the cell cycle characteristics have remained unknown. However, the *M. jannaschii* genome was shown to contain a remarkable mixture of genes with similarities to cell cycle genes from both the *Bacteria* and *Eucarya* domains. (Cell cycle genes are here defined as those involved in chromosome replication, nucleoid processing, or cell division.) This observation suggests that studies of the archaeal cell cycle may increase the understanding not only of the archaea but also of organisms from the other domains (3). Thus, it is of interest to determine if the apparent mix of features from the other two domains is paralleled also in the cell cycle characteristics, or if the archaea contain unique cell cycle features that distinguish them from other organisms.

In flow cytometry analysis of exponentially growing cells, the cell cycle of both prokaryotes and eukaryotes is distinguished as a series of stages, each of which is characterized by a particular cellular DNA content (Fig. 1). The first stage (B period in eubacteria; usually G_1 in eukaryotes) starts with the generation of a newborn cell at cell division and lasts until initiation of chromosome replication. During this stage, the DNA content of the cells is at its lowest and remains constant, such that a peak is seen at the left end of the DNA content distribution. The next stage is the chromosome replication period (C period in eubacteria; S phase in eukaryotes), during which the DNA content gradually increases to the 2N amount, forming a ridge in the DNA content distribution. After this follows the stage from termination of replication until completion of cell division (D period in eubacteria; usually encompassing G_2, M, and cytokinesis in eukaryotes), during which chromosome segregation and nucleoid partition (mitosis and nuclear division in eukaryotes) take place. The DNA content is here at its highest and again remains constant such that a second peak, at the right end of the distribution, is formed. The relative lengths of the cell cycle periods can be deduced from the shape of the DNA content distribution. A long B (G_1) period yields a high first peak, whereas a long postreplication period results in a high second peak. There are exceptions in which the conversion of the DNA content distribution into cell cycle periods is more complex, e.g., in fast-growing *Escherichia coli* cells, in which replication cycles may overlap (19), and in the fission yeast *Schizosaccharomyces pombe*, in which S phase may begin before cytokinesis is complete (8).

In stationary phase, the number of chromosome equivalents in eubacterial cells is dependent on the growth rate during the previous exponential phase (1). Thus, in fast-growing *E. coli* cells, several rounds of chromosome replication are simultaneously in progress and stationary-phase cells contain many genome equivalents, whereas the majority of a population of slowly growing cells end up with one genome equivalent in stationary phase. Eukaryotic cells that exit from the cell cycle into a resting stage (G_0) usually do so from the G_1 phase, although there are examples of cells that enter from G_2 (5).

Here, we report the first cell cycle analysis of archaea. We have measured the DNA content distributions of thermophilic archaea both in the exponential and stationary growth phases and have determined the lengths of the different cell cycle periods. Light scatter was also recorded, and we observed changes that reflect differences in size, morphology, and/or composition between cells in different growth phases.

MATERIALS AND METHODS

Strains. Type strains *Sulfolobus acidocaldarius* DSM 639 and *Sulfolobus solfataricus* DSM 1616 were purchased from the Deutsche Sammlung von Mikroorganismen und Zellkulturen, Braunschweig, Germany. *S. solfataricus* MT4 (7) and *S. acidocaldarius* DG64 (11) were kindly provided by Francesca Pisani and Dennis Grogan, respectively.

Growth conditions. The growth medium described by Grogan (10), i.e., Allen mineral base supplemented with 0.2% tryptone, was used. The pH of the final medium was around 3.0 (no pH adjustment was done). Solid medium was obtained by the addition of 0.5% Gelrite (Merck and Co.) gellan gum, 10 mM $MgSO_4$, and 2.5 mM $CaCl_2$ (final concentrations).

At the start of each experiment, the strains were streaked from stocks stored at −70°C in 10% dimethyl sulfoxide onto solid medium and incubated for 7 days

* Corresponding author. Mailing address: Department of Microbiology, Box 581, Biomedical Center, Uppsala University, S-751 23 Uppsala, Sweden. Phone: 46-18-471 40 58. Fax: 46-18-53 03 96. E-mail: Rolf.Bernander@bmc.uu.se.

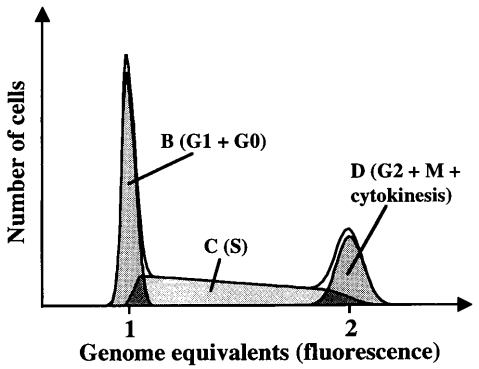

FIG. 1. Theoretical DNA content distribution. In flow cytometry, cells stained with a DNA-specific stain are individually analyzed, and the strength of the fluorescence signal is proportional to the intracellular DNA content. Cells that were in different cell cycle periods at the time of sampling form overlapping distributions, as illustrated. Importantly, the absolute height of a peak is arbitrary and depends on the scaling factor: it is the height of the peaks relative to each other and the general shape of the distribution that is of importance.

at 76°C in plastic bags. For each strain, three to four colonies from a plate were used to inoculate a 15- to 20-ml liquid culture in a 100-ml Erlenmeyer flask. The flasks were sealed tight to avoid evaporation: no special effort was made to increase the aeration. Growth was monitored by measuring optical density at 600 nm. The cultures were grown to stationary phase at 79°C in a shaking water bath (model PL-50; Heto-Holten A/S). The stationary-phase cultures were diluted about 10^4-fold (*S. solfataricus*) or 10^6-fold (*S. acidocaldarius*) into 15 ml of fresh growth medium in 100-ml flasks and grown until an optical density of 0.1 to 0.15 was reached. The cultures were again diluted about 20- to 30-fold (*S. solfataricus*) or 200- to 300-fold (*S. acidocaldarius*) into fresh medium in 500-ml flasks containing 75 ml of growth medium and then grown for an additional 24 h. At this point, an optical density of about 0.1 was usually reached, and the cultures were sampled for flow cytometry.

To obtain stationary-phase cells, the cultures were incubated for at least an additional 24 h after the optical density had ceased to increase. Disappearance of the B- and C-period populations from the DNA content distributions was taken to indicate that stationary phase had been reached.

Sample treatment and DNA staining. Samples for flow cytometry were collected by pipetting aliquots from the cultures directly into ice-cold ethanol (70%, final concentration).

A variety of sample treatment protocols were tested, including variation of the pH of the various solutions since the strains grow at low pH, but no significant improvement was found over standard protocols used for *E. coli* cells (reviewed in reference 19). Thus, before DNA staining, the cells were centrifuged in a bench-top centrifuge at 13,000 rpm for 5 min. The supernatants were removed by aspiration, and some liquid was always kept to avoid aspirating away the often loose pellets. The cells were washed in 1 ml of a buffer containing 10 mM Tris (pH 7.5) and 10 mM $MgCl_2$, centrifuged again, and resuspended in an appropriate volume of the same buffer. The samples were kept cold at all steps, and vortexing was avoided. All solutions were filtered through 0.2-μm-pore-size filters to remove particles that contribute to light scatter background noise.

Enzymatic treatments were performed in water baths at 37°C at the following enzyme concentrations: proteinase K, 50 μg/ml; RNase A, 100 μg/ml; and DNase I, 15 U (1 U degrades 1 μg of DNA in 10 min). The suspensions were gently inverted after 30 min to resuspend sedimented cells. After 60 min, the cells were washed in 0.5 ml of buffer and resuspended as described above.

DNA staining was performed by mixing 65 μl of cells of appropriate concentration with 65 μl of staining solution in the same buffer. The final concentrations of the different DNA stains were as follows: ethidium bromide, 20 μg/ml; mithramycin A, 100 μg/ml; 4′,6-diamidino-2-phenylindole (DAPI), 1 μg/ml; and Hoechst 33258, 1 μg/ml. The stained cells were kept on ice for about 60 min before analysis.

Flow cytometry. Sample analysis was performed with a Bryte HS flow cytometer (Bio-Rad). Through a system of interchangeable filter blocks, the instrument could be used for all three stains tested. Instrumentation, sample preparation, and analysis have been reviewed by Skarstad et al. (19), and flow cytometry in general has been reviewed by Shapiro (18).

Due to the small genome size and the weak light scatter signals generated by the cells, the analyses required careful instrument calibration, performance, and monitoring. The commercially supplied version of the instrument was modified by installing a mercury arc lamp as the light source. Plastic beads of uniform size and fluorescence were used for calibration and adjustment. The beads were labelled with different coumarin dyes and were either 1.5 μm in diameter (Bio-Rad) or 1.0 μm in diameter (Polysciences). *E. coli* standard samples of known properties were always run prior to the archaeal samples to ensure that distributions of high resolution and sensitivity were obtained.

For a signal to be recorded by the flow cytometer, a threshold needs to be set for either the light scatter or the fluorescence parameter, such that only if a signal is above this threshold will it be recorded. Whenever possible, a light scatter threshold was used (i.e., DNA-less cells would be recorded if present). After treatment with proteinase A, and for stationary-phase cells, this was not possible due to a substantial overlap between the light scatter signals from the cells with background noise; a fluorescence threshold was then used. As a result of this choice, the positions of the background noise peak in the histograms in Fig. 2 and 6 differ depending on which threshold was used. Between 20,000 and 50,000 cells were analyzed in each sample, and a resolution of either 256 or 1,024 channels was used for data storage.

Cell cycle analysis. The experimentally obtained DNA content distributions were transferred into the ModFit computer software (Verity Inc.) for cell cycle analysis, and simulations were performed until good fits were obtained between the experimental data and the theoretical simulations. Compromises had to be made during the simulations: the best fits were obtained with simulations in which it was assumed that there was a slight element of nonlinearity in the fluorescence axis. Simulations in which absolute linearity was assumed always resulted in no B-period population at all being obtained, and the area around the left end of the DNA distributions became flat instead of showing a small peak. The deviation from linearity was minor: the mean of the D (G_2) peak divided by the mean of the B (G_1) peak was between 1.85 and 1.95 instead of 2.0. Flow cytometry and cell cycle analysis have been reviewed and discussed by Rabinovitch (16) and Skarstad et al. (19). However, all considerations may not be applicable to archaea.

To calculate the relative lengths of the cell cycle periods, the exponential age distribution was taken into account (the fact that there are twice as many new-born cells as dividing cells in an exponentially growing population, which, if not compensated for, results in an overestimation of the length of the B period and an underestimation of the length of later periods). The fraction of cells in the different cell cycle periods (from the theoretical simulations) was converted to the cell age at the start of each period, using formula A5 in reference (21). The cell age at the start of the C period was used to calculate the relative length of the B period, and the length of the C period was obtained by subtracting this value from the combined lengths of C and D, which were calculated from the initiation age at the start of the D period. The D period occupied the remainder of the cell cycle.

In the different simulations and calculations, it is assumed that the rate of DNA replication is constant during a round of replication and that cell growth is exponential during the cell cycle. These assumptions have not been experimentally addressed for archaea.

RESULTS

Proteinase, RNase, and DNase treatments. We wanted to demonstrate that DNA staining protocols could be applied to archaeal cells without causing extensive cell lysis, leakage of DNA out of the cells, or DNA breakdown to an extent that would prevent flow cytometry analysis. We also wanted to show that the light scatter and fluorescence parameters indeed represented the cell mass and DNA content of these organisms. Cells of the thermophilic species *S. solfataricus* and *S. acidocaldarius* were fixed, washed, treated with different enzymes, stained with MEB, and analyzed by flow cytometry.

A control sample that had not been subjected to enzyme treatment demonstrated that *S. solfataricus* cells were intact enough after fixation and DNA staining to generate a DNA content (fluorescence) distribution that was well separated from background noise (Fig. 2B) despite the small genome size (17). The cell size (light scatter) distribution showed a minor overlap with the background (Fig. 2A). Furthermore, very few cells with a DNA content of more than two genome equivalents were observed (to the right of the highest peak), showing that there were few aggregated cells in the sample which facilitates cell cycle analysis considerably.

After treatment with proteinase K, the light scatter was reduced in strength to background level (Fig. 2C), whereas the fluorescence was largely unaffected (Fig. 2D). Cells of the *Sulfolobus* genus are surrounded by a protein-based S-layer which is similar in overall structure between species (differences are found in high-resolution analyses [15]). However, the proteinase treatment did not dramatically affect the integrity of

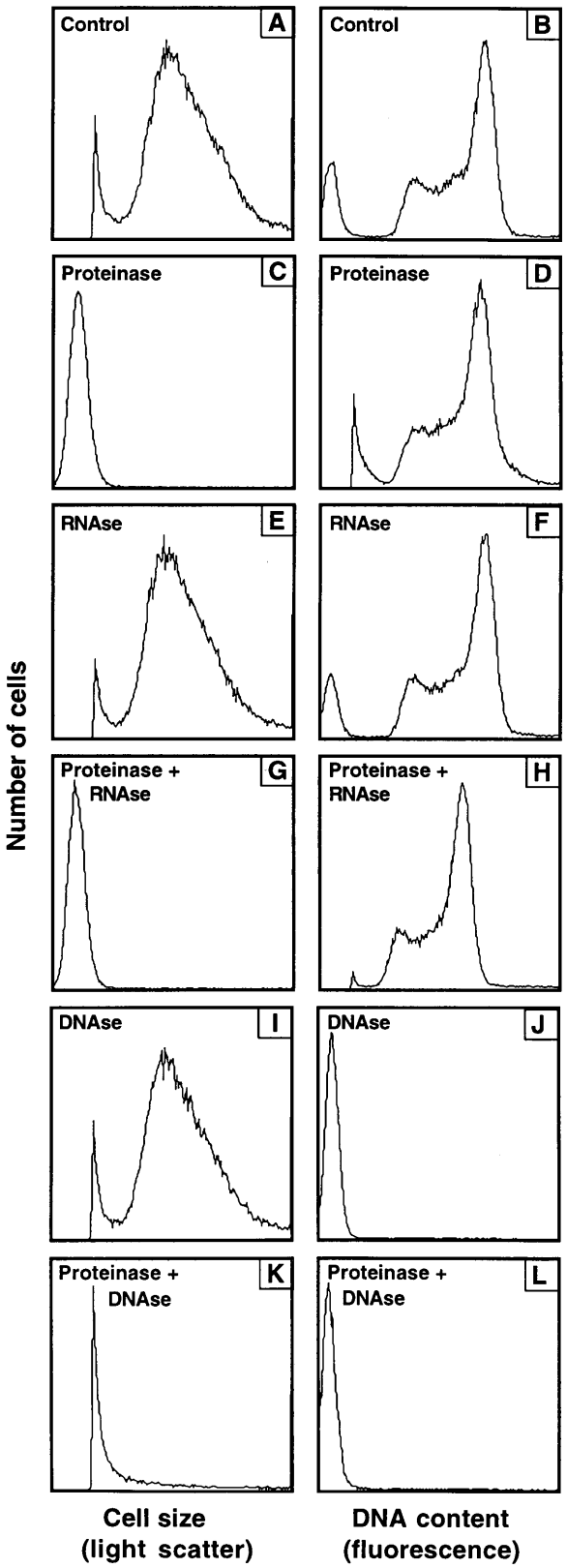

FIG. 2. Enzymatic treatments of fixed *S. solfataricus* cells. The strain was grown exponentially, and samples were fixed in ethanol. Before DNA staining with MEB and flow cytometry analysis, the cells were washed, resuspended in buffer, and treated with the indicated enzymes for 60 min at 37°C. The untreated control (no enzyme added) in panels A and B was incubated at 37°C along with the other samples. In all panels, the peak resulting from background noise has been retained to show that it is well resolved from the signals generated by the cells. The position of the noise peak depends on which parameter was chosen for setting the threshold above which a signal should be recorded (see Materials and Methods).

the S-layer (12) since the cells were still intact enough to keep from lysing and DNA leakage. Thus, the proteinase may have acted mainly on internal protein, which constitutes the bulk of cellular mass, thereby altering the light scatter properties of the cells. In fluorescence microscopy analysis, the cells showed a ghost-like appearance while retaining strong intracellular fluorescence (not shown).

Treatment with RNase A had little effect on either parameter (Fig. 2E and F). Combined proteinase and RNase treatment (Fig. 2G and H) reduced the strength of the fluorescence signal somewhat, but the shape of the distribution was retained. Thus, the proteinase treatment presumably increased the penetration of the RNase into the cells, and since the fluorescence signal strength was only slightly affected, stain bound to cellular RNA contributed to the fluorescence only to a minor extent.

In accordance, DNase I treatment eliminated the fluorescence signal almost completely, without affecting the light scatter (Fig. 2J and I), and combined DNase I and proteinase treatment extinguished both signals (Fig. 2K and L).

We conclude that the light scatter and fluorescence signals were strongly dependent on cellular protein and DNA, respectively. The results obtained with *S. acidocaldarius* were essentially the same (not shown).

Effects of different DNA stains. DNA staining efficiency may vary between stains due to differences in their penetration into the cells. Different stains also bind to DNA in different manners, and it is conceivable that the organization of the chromosome DNA can affect the binding of a stain (below). Therefore, if the DNA content histogram remains similar even though different stains are used, this indicates that the overall shape and relative distribution are not distorted by the particular organization of the chromosome DNA or by a low staining efficiency.

A range of stain concentrations were first tested to ensure that the DNA was saturated with stain at the concentrations finally chosen (not shown). The DNA content distributions of both strains were found to be similar whether the cells were stained with MEB (Fig. 2B; see also Fig. 4), DAPI (Fig. 3A and C), or Hoechst 33258 (Fig. 3B and D). We conclude that the fluorescence distributions reflected the true DNA content distribution in the cell populations and could therefore be used for cell cycle analysis.

Genome size estimations and in vivo chromosome DNA organization. Genome size can be estimated by flow cytometry by comparing with cells of known genome content. The published values for *S. solfataricus* (17) and *S. acidocaldarius* 7 (14) (neither strain is identical to the type strains used here) are 3.1 and 2.7 Mb, respectively. In all experiments, the genome of *S. acidocaldarius* was found to be significantly smaller than that of *S. solfataricus*, as demonstrated in Fig. 3, and the relative difference was always similar. Thus, the relative genome sizes could conveniently be estimated with this method.

E. coli cells containing only fully replicated chromosomes, obtained by treatment with rifampin or by using stationary-phase cultures (19), were used to calibrate the fluorescence axis. However, with the MEB stain, the genome sizes of the archaea were underestimated with this approach (not shown). The ethidium bromide component of the stain is an interca-

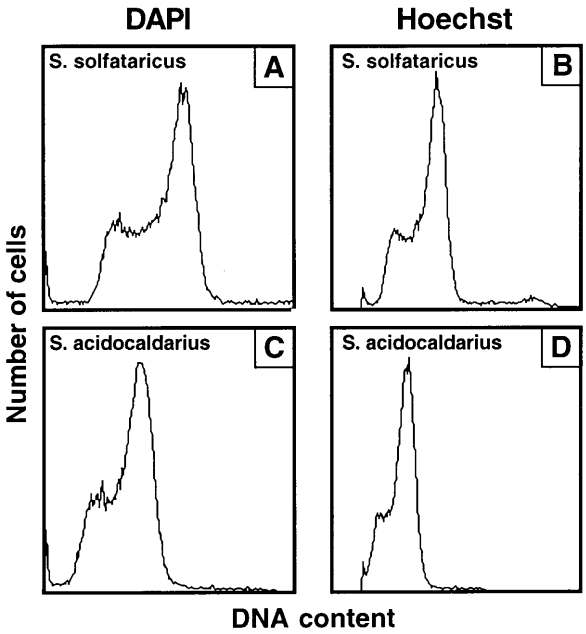

FIG. 3. Alternative DNA staining. The two strains were grown exponentially, and samples were collected and fixed in ethanol. The cells were stained with DAPI or Hoechst 33258 at a final concentration of 1 μg/ml and analyzed by flow cytometry.

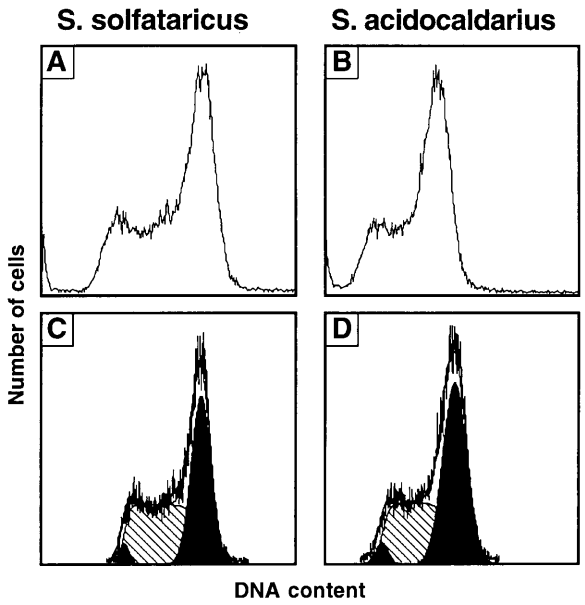

FIG. 4. Cell cycle analysis of archaea by flow cytometry. The strains were grown exponentially, and samples were collected and fixed in ethanol. The cells were stained with MEB and analyzed by flow cytometry (A and B). The resulting DNA distributions were analyzed with the ModFit software. Examples of computer simulations which fitted the experimental data are shown in panels C and D. The B and D populations are shown as filled areas, and the C population is striped. The combined fit is drawn as a solid line on top of the experimental distribution and is therefore difficult to distinguish.

lating dye which is routinely used to analyze DNA topology and the level of supercoiling, including differentiation between negative and positive supercoiling (reviewed in reference 2). It is likely that there are differences in the in vivo organization of the chromosome DNA between *E. coli* and thermophilic archaea, as evidenced by the presence of reverse gyrase activity (which introduces positive supercoiling) only in the latter (9). Thus, differences in chromosome supercoiling probably resulted in different relative amounts of ethidium bromide being bound to the *Sulfolobus* and *E. coli* DNAs. Size estimations in assays using the DAPI and Hoechst 33258 dyes, which do not intercalate (6), differed by less than 15% from the expected values, confirming that the peaks indeed represented one and two chromosomes in the archeal species.

The results showed that different stains can be used as tools to probe for differences in DNA structure and chromosome organization between cells. Also, relative genome size estimations between related species can readily be obtained. However, accurate absolute size estimations require that the scale be calibrated with a related species for which the chromosome organization and staining efficiency are similar.

Cell cycle analysis of *S. solfataricus* and *S. acidocaldarius*. The strains were grown in batch cultures at 79°C for more than 10 doubling times and then diluted such that they had been growing for a minimum of 24 h before sampling. The doubling times were determined to 425 and 213 min for *S. solfataricus* and *S. acidocaldarius*, respectively, under the growth conditions used. The DNA content distribution of exponentially growing *E. coli* cells varies significantly with optical density in rich medium and to a lesser extent in poorer media (1). Samples were therefore collected from different optical densities (0.02, 0.1, and 0.2) to ensure that the DNA distributions did not vary with cell concentration.

DNA content distributions were gathered (Fig. 4A and B) in repeated experiments using different stains as described above and analyzed with the ModFit software to produce optimal fits between the experimental and theoretical distributions (exemplified by Fig. 4C and D). From this, the proportion of cells in the different cell cycle periods were obtained, and the relative lengths of the cell cycle periods were then calculated as described in Materials and Methods.

The estimated length of the B period did not exceed 5% of the cell cycle in either strain in the simulations and was usually 3% or shorter. The estimations of the relative lengths of the C and D periods depended somewhat on the choice of parameters in the theoretical simulations (see Materials and Methods). Furthermore, for *S. solfataricus*, the experimental DNA content distributions were similar regardless of the optical density at sampling, whereas there was minor sample-to-sample variation for *S. acidocaldarius* (not shown). Bearing these considerations in mind, the relative lengths of the C and D periods were estimated to occupy 37% (157 min) and 60% (255 min) of the cell cycle, respectively, for *S. solfataricus*. A test with *S. solfataricus* MT4 indicated that the cell cycle characteristics were similar in this strain (not shown). For *S. acidocaldarius*, the C period was estimated to last between 26 and 40% (55 to 85 min) of the cell cycle, and the D period was estimated to last between 58 and 72% (124 to 153 min). Also, *S. acidocaldarius* DG64 was grown at 70°C, at which temperature the doubling time was about 6 h; also under these conditions, the postreplication stage dominated the cell cycle (not shown).

Little is known about the in vivo replication characteristics of archaea, and therefore the accuracy of the computer simulation of the shape of the C-period (S-phase) distribution is difficult to estimate. The overall conclusion was clear, i.e., the B period was very short and the replication and postreplication stages were long (further evidence is given below), but the length of the C period should be treated as an approximation

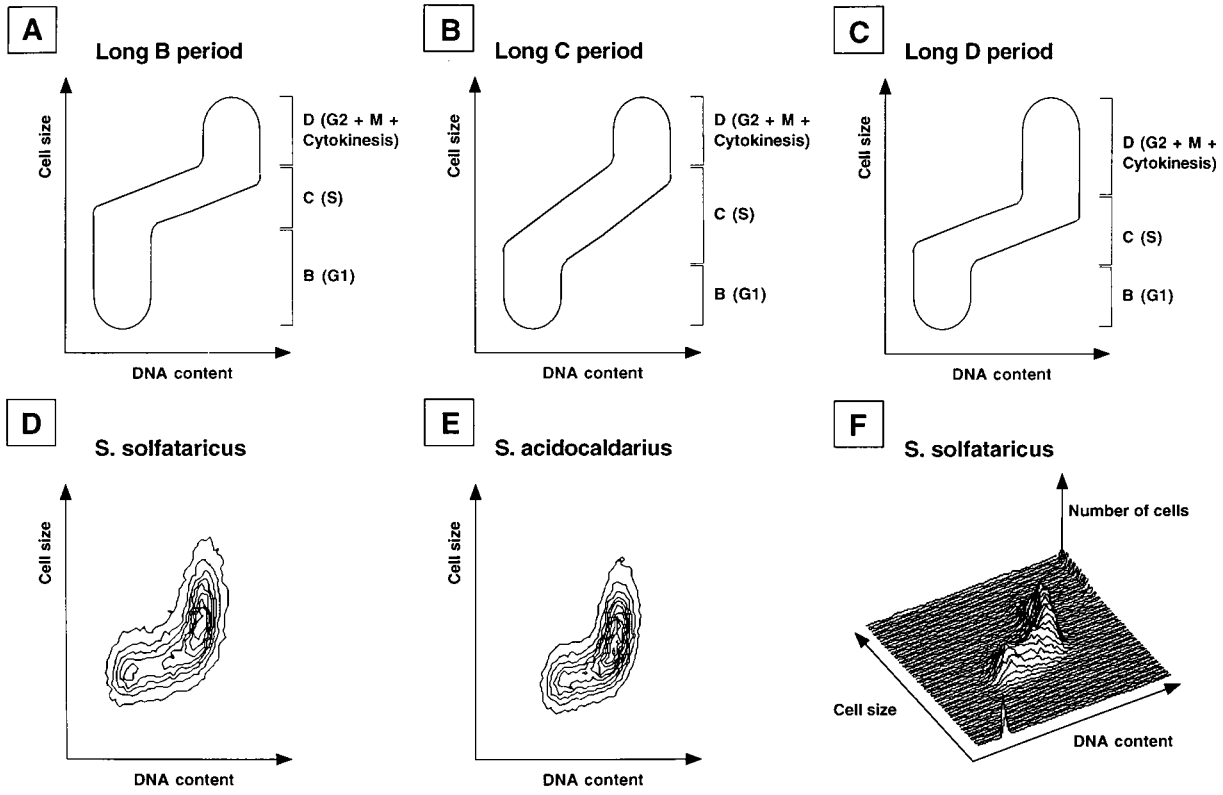

FIG. 5. Combined cell size (light scatter) and DNA distributions viewed from above. Newborn cells are located at the lower left in each distribution and travel rightward and upward as they pass through the different cell cycle stages. Thus, an old cell that is about to divide is located at the upper right in each distribution and will generate two cells that again appear at the lower left. (A to C) Theoretical representations that illustrate the characteristic shapes of distributions that result from cells having long B, C, and D periods, respectively; (D to F) experimental data from the same samples that were used to generate Fig. 4.

until the in vivo replication characteristics have become better understood.

Correlation between cellular mass and DNA content. Figures 5A to C show theoretical representations of combined light scatter and DNA content distributions for cells with different relative lengths of the cell cycle periods. Characteristic differences in the patterns are apparent depending on whether it is the B, C, or D period that dominates in the cell cycle. In Fig. 5D and E, the experimental results obtained with *S. solfataricus* and *S. acidocaldarius* are shown. The shapes of the distributions are an extreme case of Fig. 5C, i.e., a very short B period in combination with a long postreplication period, in agreement with the analyses of the DNA content distributions alone (see above). In these analyses, there was also an extensive overlap between the B and C period populations (Fig. 4C and D). This interpretation is strengthened in the combined light scatter and fluorescence distributions, in that no distinct B-period populations could be distinguished. The C-period population extended right down to the lower left end of the distributions, showing that replication started shortly after division (Fig. 5D and E; cf. Fig. 5A to C, in which B-period populations are drawn). The *S. solfataricus* distribution is also plotted in a three-dimensional representation (Fig. 5F), in which the progression through the cell cycle is differently illustrated, and may be followed by tracing the ridge from the lower left to the upper right part.

Flow cytometry analysis of stationary-phase cultures. The cultures were allowed to reach stationary growth phase, after which they were sampled for flow cytometry. For both strains, only the rightmost peak was retained in the DNA content distributions (Fig. 6), showing that all cells contained two genome equivalents in stationary phase under these growth conditions. When the MEB stain was used, the peak was positioned somewhat to the left of the two-chromosome peak obtained for the exponentially growing cultures, as illustrated with *S. solfataricus* in Fig. 6B and D. In parallel, the light scatter signal was considerably reduced (Fig. 6A and C). We have performed a combined phase-contrast–epifluorescence microscopy analysis of the cells (14a) and confirmed that cellular size is reduced upon entry into stationary phase. Also, after ethanol fixation, stationary-phase cells were more transparent than exponentially grown cells, indicating that the reduction in light scatter in the flow cytometry analysis probably reflected changes both in cell size and in composition.

When the DAPI or Hoechst 33258 stain was used, the position of the two-chromosome peak coincided better with the corresponding peak in the exponential distribution, as illustrated for *S. acidocaldarius* in Fig. 6E to L. Thus, the differences in peak position for the various stains again appeared to reflect differences in chromosome organization, but this time between actively growing and stationary-phase cells. The MEB staining efficiency was apparently more affected by these differences than that of DAPI and Hoechst 33258, again presumably because only the MEB stain contains an intercalating dye (see above). The stationary-phase *S. acidocaldarius* cells showed a slight tendency to aggregate, evident as minor peaks and a trail to the right of the major peak in Fig. 6H and L. A reduction in light scatter was again observed in stationary

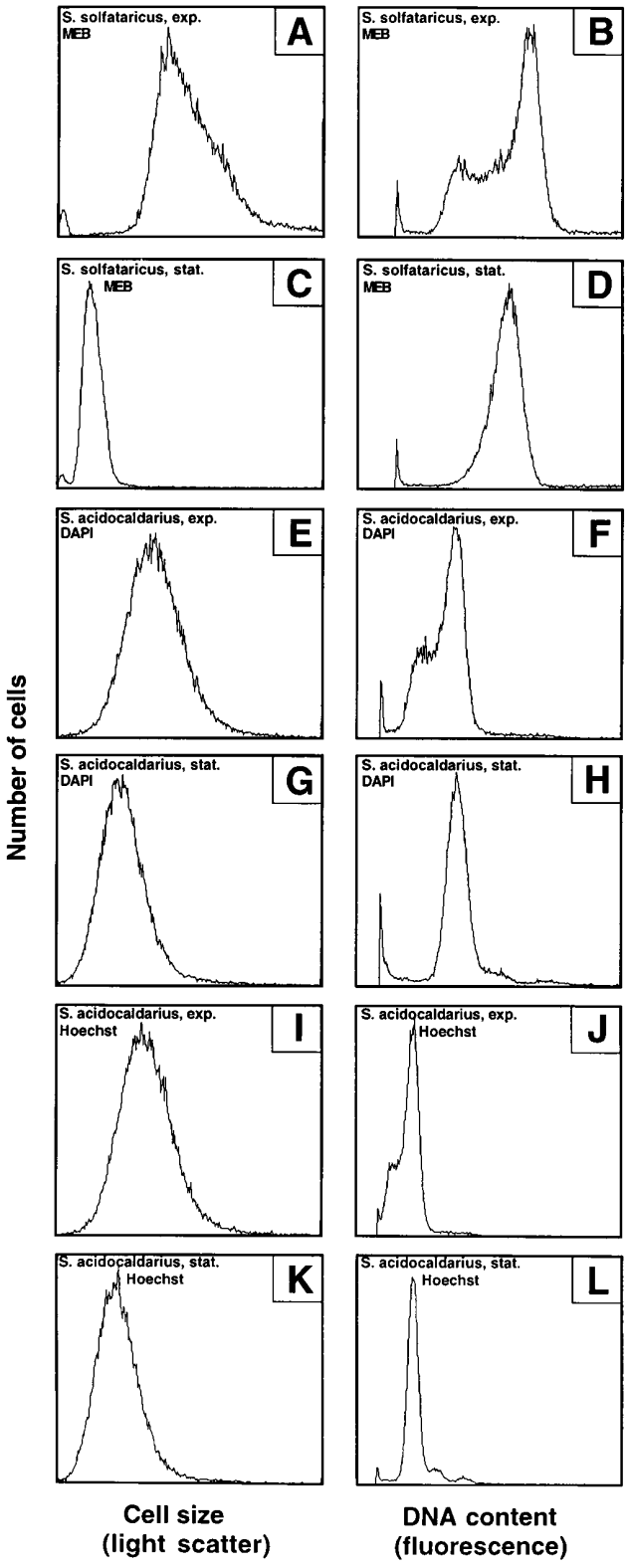

FIG. 6. Flow cytometry analysis of stationary-phase archaeal cultures. Cultures of *S. solfataricus* (A to D) and *S. acidocaldarius* (E to L) were grown exponentially until stationary phase was reached. Samples for flow cytometry were collected from the exponential (exp.; A, B, E, F, I, and J) and stationary (stat.; C, D, G, H, K, and L) growth phases. Staining with MEB (A to D), DAPI (E to H), or Hoechst 33258 (I to L) is illustrated. The positions of the various peaks can be compared only for each stain internally, since different instrument settings were used for the stains.

phase, but this was less dramatic than when the MEB stain was used, in accordance with the poor light scatter sensitivity of the Bryte instrument in the UV wavelength range compared to the visible range (3a).

In conclusion, the cells accumulated with a two-chromosome genome content in stationary phase in both species, accompanied by changes in cell size and composition.

DISCUSSION

We have carried out the first cell cycle analysis of organisms from the *Archaea* domain, and this is also the first time that the cell cycle of thermophilic organisms has been characterized. In short, the analyses showed that both *S. solfataricus* and *S. acidocaldarius* initiated chromosome replication shortly after cell division and that the replication and postreplication stages of the cell cycle were long. Cells in stationary phase contained two genome equivalents and gave rise to significantly less light scatter than exponentially growing cells.

Although archaea are believed to be more closely related to eukaryotes than to eubacteria, they are still prokaryotes. Therefore, we choose to apply the terminology used for the prokaryotic cell cycle (B, C, and D periods; see the introduction). This also appears appropriate as the G_1, S, G_2, and M terminology was developed for cells that go through mitosis and nuclear separation, processes that in the archaea are absent or presumably more similar to the corresponding eubacterial events.

The precise growth rate and cell cycle characteristics of a population are influenced by a variety of parameters (the particular strain chosen, medium composition, incubation temperature, aeration, etc.). These parameters vary between experiments and laboratories, and the absolute lengths of the cell cycle periods are therefore always approximations. The relative lengths of the periods are presumably more general, i.e., a short B period together with long C and D periods. In contrast, in *E. coli* strains growing slowly, the D period is the shortest part of the cell cycle and the prereplication period is long (13). Fission and budding yeast are among the few organisms that display the combination of a relatively short G_1 (B) period and a long postreplication period (8). Interestingly, genes similar to yeast genes (encoding cdc21, CDC54, CBF5, and Lpg15) putatively involved in the cell cycle have been identified in the *M. jannaschii* genome (4).

The C-period lengths of the thermophilic archaea were in the same range as for *E. coli* at low growth rates (13). (There may exist growth conditions at which shorter doubling times can be attained for *Sulfolobus* strains, and in analogy to *E. coli*, the rate of replication might then be higher.) The archaeal genomes are 35 to 45% smaller than that of *E. coli*, and a shorter replication time would therefore be expected (disregarding differences in growth temperature, DNA polymerase efficiency, etc.). Therefore, we believe that the relatively long time required for replication indicates that there is only a single replication origin per chromosome in these organisms, as in *E. coli.*

The organization of the chromosome DNA in exponentially growing cells appeared to differ from that of *E. coli*, as revealed by the difference in the relative fluorescence for the intercalating and nonintercalating dyes in the archaea and in *E. coli*. Hyperthermophilic archaea contain reverse gyrase, which introduces positive supercoils into DNA. This is therefore an indication that the in vivo topological organization of the chromosome DNA in these organisms is indeed different from that of organisms that lack reverse gyrase.

Cells resting in stationary phase contained two genome

equivalents. Although *E. coli* cells may end up with more than one chromosome in stationary phase under certain conditions (1), the mechanism is different. If growth is rapid during the exponential growth phase, several overlapping rounds of replication are in progress at the same time. When the cells reach stationary phase, they are unable to go through enough successive divisions to end up with only one chromosome per cell, since cellular growth stops before all divisions have been carried out. Therefore, there is a mixture of cells containing, e.g., one, two, or four fully replicated chromosomes in the population, depending on the cell cycle stage at which the cells entered stationary phase. However, the slower growth is in exponential phase, the higher is the proportion of the population that ends up with only a single chromosome. At the growth rates of the *Sulfolobus* species discussed in this report, most *E. coli* cells end up with a single chromosome in stationary phase. Thus, the prereplication stage is preferred as the resting stage in this organism. In the *Sulfolobus* species, no cells ended up with one chromosome despite the slow growth. Thus, and in contrast to *E. coli*, exit into the resting stage occurred exclusively in the postreplication period.

A reduction in light scatter was also observed in stationary phase, which indicates that the cells became smaller, as is the case for *E. coli* cells entering stationary phase (1). However, in light microscopy analysis, the reduction in size appeared somewhat less dramatic. Light scatter is a complex parameter which is influenced not only by cell size but also by shape and composition. The reduction may therefore have been due to, in addition to a size decrease, changes in cell morphology and composition as the cells left exponential growth.

These organisms are, to our knowledge, those with the smallest genomes whose cell cycles have been analyzed by flow cytometry. This study extends the range of organisms that such analyses can be performed on, perhaps even to include the prokaryotes for which the entire genome sequence has been determined (genome sizes of <2 Mb) and for which the entire repertoire of cell cycle genes therefore is available.

Different archaeal groups branch deeply within the evolutionary tree, and archaea display a variety of cell morphologies and are found in extremely different habitats. Thus, it appears unlikely that the cell cycle features of the species studied in this report will be general for the *Archaea* domain, particularly in light of the wide variety of cell cycle characteristics that are found within the other two domains. A short B period, long D period, and postreplication resting stage might be characteristic of thermophiles, but a broader range of species need to be studied to verify this suggestion. It will be necessary to analyze the cell cycle characteristics of a large variety of archaea to get an overview of the spectrum of cell cycles among these unique organisms and to be able to generalize about archaeal life styles. Thus, cell cycle investigations will remain an interesting research field for further studies of the *Archaea* domain.

ACKNOWLEDGMENTS

We thank Dennis Grogan and the groups of Karl Stetter and Harald Huber for guidance on the cultivation of thermophilic archaea and Kirsten Skarstad for discussions relating to the cell cycle.

This work was supported by the Swedish Natural Science Research Council and the Swedish Foundation for Strategic Research.

REFERENCES

1. **Åkerlund, T., K. Nordström, and R. Bernander.** 1995. Analysis of cell size and DNA content in exponentially growing and stationary-phase batch cultures of *Escherichia coli*. J. Bacteriol. **177:**6791–6797.
2. **Bates, A. D., and A. Maxwell.** 1993. DNA topology. IRL Press, Oxford, England.
3. **Bernander, R.** 1994. Universal cell cycle regulation? Trends Cell Biol. **4:**76–79.

3a. **Boye, E.** Personal communication.

4. **Bult, C. J., O. White, G. J. Olsen, L. Zhou, R. D. Fleischmann, G. G. Sutton, J. A. Blake, L. M. FitzGerald, R. A. Clayton, J. D. Gocayne, A. R. Kerlavage, B. A. Dougherty, J.-F. Tomb, M. D. Adams, C. I. Reich, R. Overbeek, E. F. Kirkness, K. G. Weinstock, J. M. Merrick, A. Glodek, J. L. Scott, N. S. M. Geoghagen, J. F. Weidman, J. L. Fuhrmann, D. Nguyen, T. R. Utterback, J. M. Kelley, J. D. Peterson, P. W. Sadow, M. C. Hanna, M. D. Cotton, K. M. Roberts, M. A. Hurst, B. P. Kaine, M. Borodovsky, H.-P. Klenk, C. M. Fraser, H. O. Smith, C. R. Woese, and J. C. Venter.** 1996. Complete genome sequence of the methanogenic archaeon, *Methanococcus jannaschii*. Science **273:**1058–1073.
5. **Costello, G., L. Rodgers, and D. Beach.** 1986. Fission yeast enters the stationary phase G_0 state from either mitotic G_1 or G_2. Curr. Genet. **11:**119–125.
6. **Crissman, H. A., and G. T. Hirons.** 1994. Staining of DNA in live and fixed cells. Methods Cell. Biol. **41:**195–209.
7. **De Rosa, M., A. Gambacorta, and J. D. Bu'Lock.** 1975. Extremely thermophilic acidophilic bacteria convergent with *Sulfolobus acidocaldarius*. J. Gen. Microbiol. **86:**156–164.
8. **Forsburg, S. L., and P. Nurse.** 1991. Cell cycle regulation in the yeasts *Saccharomyces cerevisiae* and *Schizosaccharomyces pombe*. Annu. Rev. Cell Biol. **7:**227–256.
9. **Forterre, P., A. Bergerat, and P. Lopez-Garcia.** 1996. The unique DNA topology and DNA topoisomerases of hyperthermophilic archaea. FEMS Microbiol. Rev. **18:**237–248.
10. **Grogan, D. W.** 1989. Phenotypic characterization of the archaebacterial genus *Sulfolobus*: comparison of five wild-type strains. J. Bacteriol. **171:**6710–6719.
11. **Grogan, D. W.** 1996. Exchange of genetic markers at extremely high temperatures in the archaeon *Sulfolobus acidocaldarius*. J. Bacteriol. **178:**3207–3211.
12. **Grogan, D. W.** 1996. Organization and interactions of cell envelope proteins of the extreme thermoacidophile *Sulfolobus acidocaldarius*. Can. J. Microbiol. **42:**1163–1171.
13. **Helmstetter, C. E.** 1996. Timing of synthetic activities in the cell cycle, p. 1627–1639. *In* F. C. Neidhardt, R. Curtiss III, J. L. Ingraham, E. C. C. Lin, K. B. Low, B. Magasanik, W. S. Reznikoff, M. Riley, M. Schaechter, and H. E. Umbarger (ed.), *Escherichia coli* and *Salmonella*: cellular and molecular biology, 2nd ed. American Society for Microbiology, Washington, D.C.
14. **Kondo, S., A. Yamagishi, and T. Oshima.** 1993. A physical map of the sulfur-dependent archaebacterium *Sulfolobus acidocaldarius* 7 chromosome. J. Bacteriol. **175:**1532–1536.

14a. **Poplawski, A., and R. Bernander.** Unpublished data.

15. **Prüschenk, R., W. Baumeister, and W. Zillig.** 1987. Surface structure variants in different species of *Sulfolobus*. FEMS Microbiol. Lett. **43:**327–330.
16. **Rabinovitch, P. S.** 1994. DNA content histogram and cell-cycle analysis. Methods Cell Biol. **41:**263–296.
17. **Sensen, C. W., H.-P. Klenk, R. K. Singh, G. Allard, C. C.-Y. Chan, Q. Y. Liu, S. L. Penny, F. Young, M. E. Schenk, T. Gaasterland, W. F. Doolittle, M. A. Ragan, and R. L. Charlebois.** 1996. Organizational characteristics and information content of an archael genome: 156 kb of sequence from *Sulfolobus solfataricus* P2. Mol. Microbiol. **22:**175–191.
18. **Shapiro, H. W.** 1995. Practical flow cytometry, 3rd ed. Wiley-Liss, New York, N.Y.
19. **Skarstad, K., R. Bernander, S. Wold, H. B. Steen, and E. Boye.** 1996. Cell cycle analysis of microorganisms, p. 241–255. *In* M. Al-Rubeai and A. N. Emery (ed.), Flow cytometry applications in cell culture. Marcel Dekker, Inc., New York, N.Y.
20. **Woese, C. R., and G. E. Fox.** 1977. Phylogenetic structure of the prokaryotic domain: the primary kingdoms. Proc. Natl. Acad. Sci. USA **74:**5088–5090.
21. **Wold, S., K. Skarstad, H. B. Steen, T. Stokke, and E. Boye.** 1994. The initiation mass for DNA replication in *Escherichia coli* is dependent on growth rate. EMBO J. **13:**2097–2102.